Supporting Information:

Polymorphic Expressions of Ultrathin Oxidic Layers of Mo on Au(111)

Taehun Lee,[†] Yun-Jae Lee,[†] Krisztián Palotás,[‡,¶,‖] Giyeok Lee,[†] Catherine Stampfl,[§] and Aloysius Soon[*,†]

[†]*Department of Materials Science & Engineering and Center for Artificial Synesthesia Materials Discovery, Yonsei University, Seoul 03722, Republic of Korea*

[‡]*Institute for Solid State Physics and Optics, Wigner Research Center for Physics, Hungarian Academy of Sciences, H-1525 Budapest, Hungary*

[¶]*MTA-SZTE Reaction Kinetics and Surface Chemistry Research Group, University of Szeged, H-6720 Szeged, Hungary*

[§]*School of Physics, The University of Sydney, NSW, 2006, Australia*

[‖]*Institute of Physics, Slovak Academy of Sciences, SK-84511 Bratislava, Slovakia*

E-mail: aloysius.soon@yonsei.ac.kr

Methodology

Computational setup for the slab model calculation

We use a supercell slab approach for the O/Mo/Au(111) system, consisting of a total of 7 to 10 atomic layers with a vacuum region of 15 Å. The Mo oxidic layers are constructed on one side of a 4 atomic layered Au(111) substrate. For atomic geometry relaxation, the bottom 2 layers of Au(111) are kept at their bulk positions and a dipole correction is applied. The Brillouin zone integrations are performed using a Γ-centered 12×12×1 grid for $p(1{\times}1)$ Au(111) substrate and equivalent **k**-point grids for the larger surface supercells. The valence configuration for the Mo, Au, and O PAW potentials are $4s^2 4p^6 4d^5 5s^1$, $5d^{10} 6s^1$, and $2s^2 2p^4$, respectively.

We note that the convergences of the Bader charges, surface work function, and the E_{SCLS} have been tested by increasing the number of grid points for the charge density integration, by varying vacuum region from 15 Å to 20 Å, and also by changing the size of the surface supercells (up to a maximum to 288 atoms in the supercell). The convergence criteria for the Bader charges, surface work function, and the E_{SCLS} is set to $0.005\,e$, 5 meV and 0.1 eV, respectively.

Ab initio atomistic thermodynamics

The average adsorption energy of oxygen atom (as taken with respect to the O_2 molecule), E^{ad} of the Mo oxidic layer on Au(111) is defined as,

$$E^{\mathrm{ad}} = \frac{1}{N_{\mathrm{O}}}\left(E_{\mathrm{O/Mo/Au}} - E_{\mathrm{Au(111)}} - N_{\mathrm{Mo}}E_{\mathrm{Mo}} - \frac{N_{\mathrm{O}}}{2}E_{\mathrm{O}_2}\right) \quad , \tag{S1}$$

where $E_{\mathrm{O/Mo/Au}}$ and $E_{\mathrm{Au(111)}}$ are the DFT-calculated total energies for O/Mo/Au(111) and pristine Au(111), respectively. N_{Mo} and N_{O} are taken as the number of Mo and O atoms in O/Mo/Au(111), while E_{Mo} and E_{O_2} are then the DFT-calculated total energies of a Mo atom in bulk Mo and the oxygen molecule, respectively. Here, E_{O_2} is corrected using the experimental binding energy of the O_2 molecule[1] to overcome the large errors as reported for GGA calculations of O_2 binding energies.[2]

To evaluate the thermodynamic stability of Mo oxidic layers on Au(111) under a reactive oxygen gas environment, the revised *ab initio* atomistic thermodynamic approach for a mildly-doped metal surface[3,4] is employed. The Gibbs free energy of adsorption (ΔG^{ad}) is defined as,

$$\Delta G^{\mathrm{ad}}(T,p) = \frac{1}{A}\left(G_{\mathrm{O/Mo/Au}} - G_{\mathrm{Au(111)}} - \Delta N_{\mathrm{Au}}\mu_{\mathrm{Au}} - N_{\mathrm{Mo}}\mu_{\mathrm{Mo}} - N_{\mathrm{O}}\mu_{\mathrm{O}}\right) \quad , \tag{S2}$$

where $G_{\mathrm{O/Mo/Au}}$ and $G_{\mathrm{Au(111)}}$ are the Gibbs free energies of O/Mo/Au(111) and pristine Au(111) with a surface area of A, respectively. μ_{Au}, μ_{O}, and μ_{Mo} are the chemical potentials of the Au, O, and Mo atoms, correspondingly. μ_{Au} is taken as the total energy of bulk Au ($E^{\mathrm{bulk}}_{\mathrm{Au}}$), since the number of Au atoms in the simulated system is assumed to be infinite in the equilibrium state with bulk Au. μ_{O} is computed with reference to half of the total energy of the O_2 molecule. ΔN_{Au} is taken as the change in the number of Au atomic species to form oxidic layers. N_{O} and N_{Mo} are then the number of O and Mo atoms in the oxidic layers, respectively.

In this spirit, various Mo/Au surface structures are considered to compute $\Delta\mu_{\mathrm{Mo}}$ with reference to the total energy of the Mo atom as,

$$\Delta\mu_{\mathrm{Mo}} = \frac{1}{N_x}(G_{\mathrm{Mo}_x\mathrm{Au}_y} - N_y\mu_{\mathrm{Au}} - N_x E^{\mathrm{atom}}_{\mathrm{Mo}}) \quad , \tag{S3}$$

where N_x and N_y are the number of atoms of Mo and Au in the $\mathrm{Mo}_x\mathrm{Au}_y$ nanocomposite system, respectively. Since the amount of Au is infinite to reach the equilibrium of the bulk phase, the assumption of μ_{Au} taken as the total energy of bulk Au ($E^{\mathrm{bulk}}_{\mathrm{Au}}$) is well-grounded.

Finally, to understand how metastable and/or kinetically-hindered oxidic surface structures may play a role in populating the actual substrate under growth conditions, the surface population, $P(n, p, T)$ of these O/Mo/Au(111) structures is computed following a Boltzmann distribution-type behaviour:

$$P(n,p,T) = \frac{\exp^{\frac{-G_n(T,p)}{\mathrm{k_B}T}}}{\sum\limits_{n=1}^{N} \exp^{\frac{-G_n(p,T)}{\mathrm{k_B}T}}} \quad , \tag{S4}$$

where $G_n(p, T)$ is the Gibbs free energy of adsorption for each surface structure, n, and it can be interpreted as a function of partial pressure (p) and temperature (T) of the O_2 molecule, and $\mathrm{k_B}$ is the Boltzmann constant. We refer readers to our previous publications for details on this approach.[2,3]

Theoretical framework to plot E_B spectra

To make a comparison with experimental XPS spectra, we calculate the theoretical E_B spectra within the DFT framework following the procedure (as illustrated in Figure S1 below):

1. For each surface structure (1L, *sh*2L, 2L, and *inv*2L), the unique oxygen atoms (O_i) which possess different chemical bonding characters, are chosen for the core-level binding energy (E_CL) calculations.

2. Using a Gaussian function centered on each O_i core-level binding energy, the E_CL curve is generated with a full width at half maximum (FWHM) of 1.00 eV to simulate the experimental XPS spectrum.

3. The relative intensity of the Gaussian function for each O_i is then set proportional to the relative surface oxygen density within the considered surface structure.

4. Lastly, to obtain the E_CL spectrum for the surface structure, the Gaussian function for O_i is then superimposed for a given surface structure.

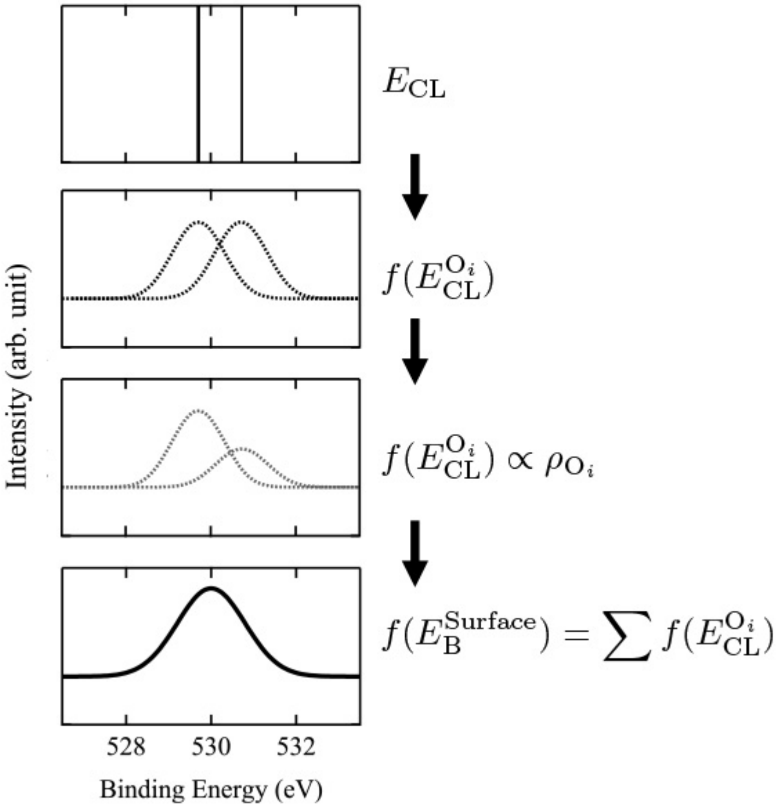

Figure S1: Procedure to plot E_{B} spectra

Figures

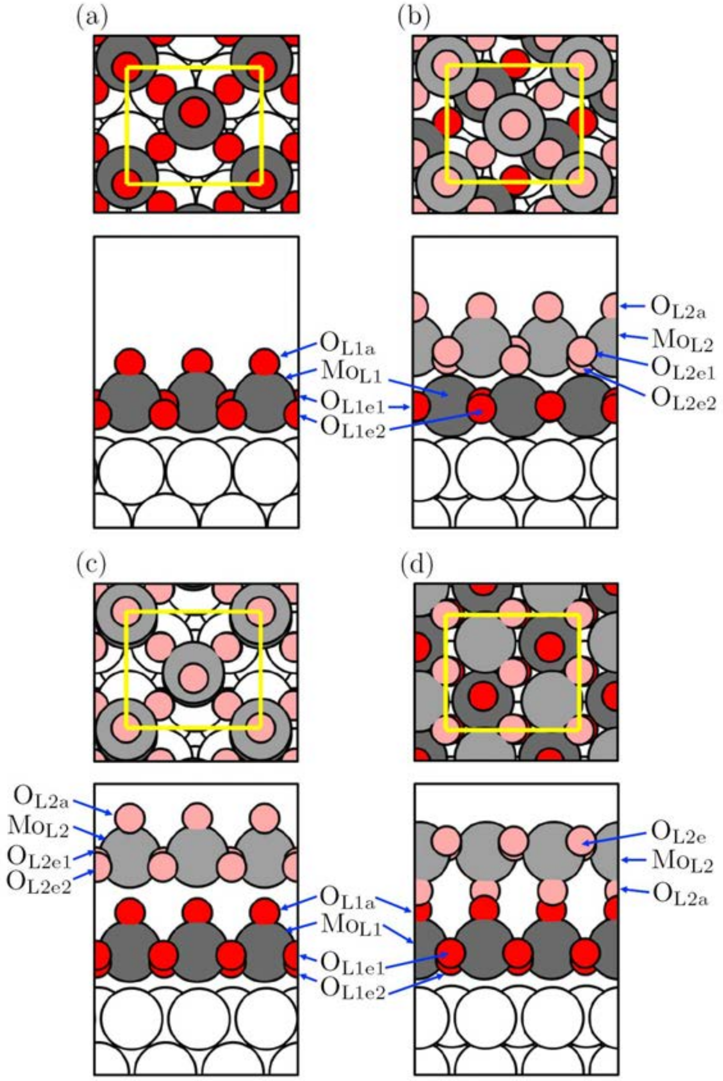

Figure S2: The various structural motifs of Mo oxidic layer on $c(4 \times 2)$ Au support.(a) 1L, (b) *sh*2L, (c) 2L, (d) *inv*2L. The dark gray, light gray, red, pink, and white spheres represent Mo atoms of the first and second layers, O atoms bonded to the Mo atoms in the first and second layers, and Au atoms, respectively. The surface unit cell is denoted as yellow solid line. The 'L', 'a', 'e' stand for the layer, axial and equatorial oxygen, e.g., O_{L2a} is the axial oxygen of second layer.

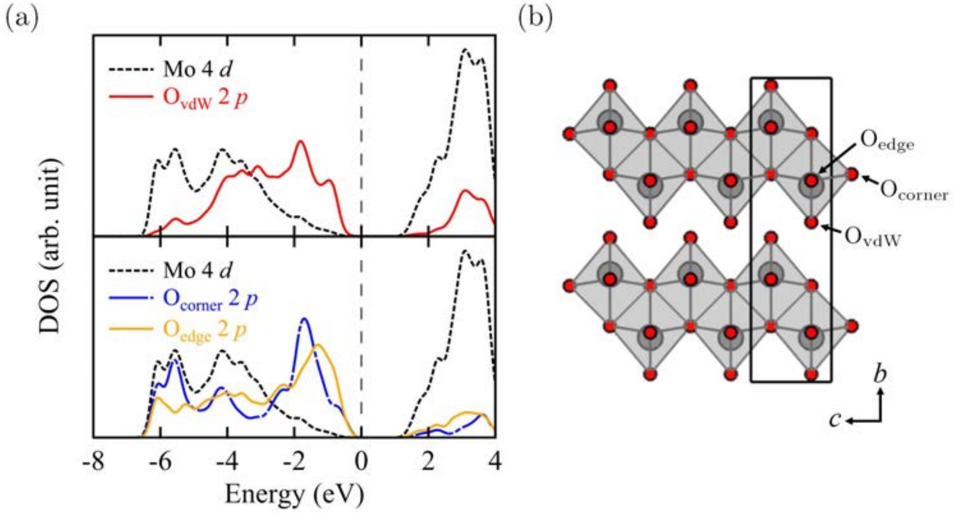

Figure S3: (a) Projected density-of-states (PDOS) for bulk α-MoO_3 of Mo $4\,d$ and O $2\,p$ states and (b) its atomic structures. The structural models are denoted with dark gray and red circles for Mo and O atoms including MoO_6 octahedron as light gray. The Fermi energy is denoted by the vertical dashed line at 0 eV.

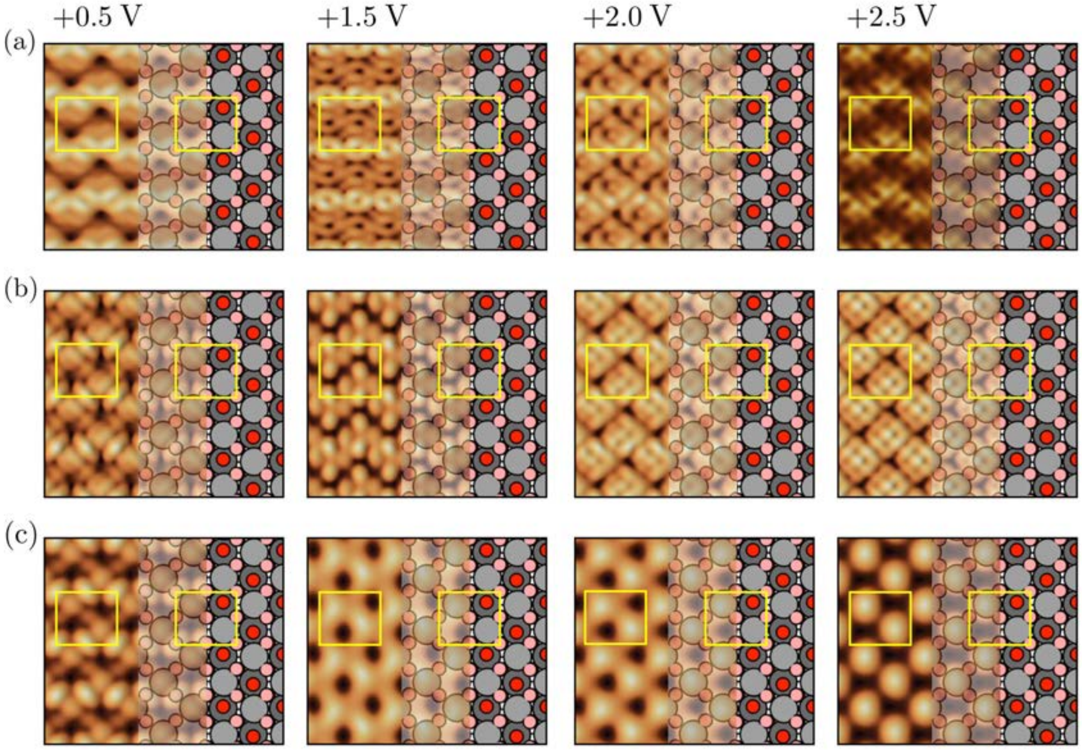

Figure S4: Simulated constant-current STM images of the *inv*2L structure for various bias voltages (+0.5, +1.5, +2.0, and +2.5 from left to right) using two types of tip model: (a) using a blunt W(110) tip with W adatom on its surface, and (b)-(c) using a blunt W(110) tip functionalized with O atom on the W adatom, at relatively high current (b) and low current (c). We refer the readers to Reference 5 for the details of the simulation.

Tables

Table S1: The real height profiles of various Mo oxidic layers of optimized structural models in this work and the apparent heights obtained in STM experiments in the cited references.

Structure	From support to top oxide layer (Å)	From bottom oxide layer to top oxide layer (Å)
1L	4.68	2.23
1L+V_O	4.76	2.23
1L+2V_O	2.75	0.27
*sh*1.5L	6.29	3.98
*sh*1.5L+V_O	4.76	2.40
*sh*2L	7.05	4.44
*sh*2L+V_O	5.48	2.93
*sh*2L+2V_O	7.04	4.63
2L	8.75	6.34
2L+V_O	6.74	4.17
2L+2V_O	8.54	6.16
*inv*2L	7.68	5.21
Reference 6	5.0	
References 7,8	5.0 − 7.0	
Reference 9	0.5, 7.0 − 13.0	

Table S2: The surface coverage of Mo (Θ_{Mo}) and O (Θ_{O}) as defined as ratio of the numbers of Mo and O atoms to the number of Au atom and the ratio of O to Mo ($N_{\mathrm{O}}/N_{\mathrm{Mo}}$) of oxidic layers.

Structure	Θ_{Mo} (ML)	Θ_{O} (ML)	$N_{\mathrm{O}}/N_{\mathrm{Mo}}$
1L	0.50	1.50	3.00
1L+$\mathrm{V_O}$	0.50	1.25	2.50
1L+2$\mathrm{V_O}$	0.50	1.00	2.00
*sh*1.5L	0.75	1.75	2.33
*sh*1.5L+$\mathrm{V_O}$	1.50	1.50	2.00
*sh*2L	1.00	2.50	2.50
*sh*2L+$\mathrm{V_O}$	1.00	2.25	2.25
*sh*2L+2$\mathrm{V_O}$	1.00	2.00	2.00
2L	1.00	3.00	3.00
2L+$\mathrm{V_O}$	1.00	2.75	2.75
2L+2$\mathrm{V_O}$	1.00	2.50	2.50
*inv*2L	1.00	3.00	3.00

Table S3: The computed surface core-level shift (E_{SCLS}, unit in eV) and theoretical binding energy (E_{B}, unit in eV) values using O 1 s state for various oxygen atoms for oxidic layer of Mo. Each E_{SCLS} and E_{B} values are calculated with respect to (w.r.t.) the different reference states. The references states of E_{SCLS} w.r.t. $E_{\mathrm{CL}}^{\mathrm{O}_{\alpha\text{-MoO}_3}}$, E_{SCLS} w.r.t. $E_{\mathrm{CL}}^{\mathrm{O}_{\mathrm{1L}}}$, and E_{B} w.r.t. $E_{\mathrm{B}}^{\mathrm{O}_{\mathrm{1L}}^{\mathrm{Exp}}}$ are averaged E_{CL} values of O 1 s state in the bulk α-MoO$_3$ (in Figure S3(b)), namely, $\mathrm{O}_{\mathrm{corner}}$, $\mathrm{O}_{\mathrm{vdW}}$, and $\mathrm{O}_{\mathrm{edge}}$, computed O 1 s state of E_{CL} value of 2L surface structure, and the experimental binding energy of 1L surface structure.[9] We note that for convenience, the labels used for the oxygen species as shown in Figure 6 of the main manuscript are tabulated in the very first column.

#	Structure	Species	E_{SCLS} w.r.t $E_{\mathrm{CL}}^{\mathrm{O}_{\alpha\text{-MoO}_3}}$	E_{SCLS} w.r.t $E_{\mathrm{CL}}^{\mathrm{O}_{\mathrm{1L}}}$	E_{B} w.r.t $E_{\mathrm{B}}^{\mathrm{O}_{\mathrm{1L}}^{\mathrm{Exp}}}$
1	1L	$\mathrm{O}_{\mathrm{L1a}}$	+0.25	+0.73	+530.73
2	1L	$\mathrm{O}_{\mathrm{L1e1}}$	−0.76	−0.28	+529.72
2	1L	$\mathrm{O}_{\mathrm{L1e2}}$	−0.79	−0.31	+529.69
3	*sh*2L	$\mathrm{O}_{\mathrm{L2a}}$	−0.08	+0.41	+530.41
4	*sh*2L	$\mathrm{O}_{\mathrm{L2e1}}$	−1.18	−0.70	+529.30
4	*sh*2L	$\mathrm{O}_{\mathrm{L2e2}}$	+0.00	+0.48	+530.48
5	*sh*2L	$\mathrm{O}_{\mathrm{L1e1}}$	−0.88	−0.28	+529.72
5	*sh*2L	$\mathrm{O}_{\mathrm{L1e2}}$	−0.76	−0.40	+529.60
6	2L	$\mathrm{O}_{\mathrm{L2a}}$	−1.07	−0.59	+529.41
7	2L	$\mathrm{O}_{\mathrm{L2e1}}$	−1.79	−1.31	+528.69
7	2L	$\mathrm{O}_{\mathrm{L2e2}}$	−1.79	−1.31	+528.69
8	2L	$\mathrm{O}_{\mathrm{L1a}}$	+0.28	+0.76	+530.76
9	2L	$\mathrm{O}_{\mathrm{L1e1}}$	−0.77	−0.30	+529.70
9	2L	$\mathrm{O}_{\mathrm{L1e2}}$	−0.78	−0.29	+529.71
10	*inv*2L	$\mathrm{O}_{\mathrm{L2e}}$	+0.64	+1.12	+531.12
11	*inv*2L	$\mathrm{O}_{\mathrm{L2a}}$	+1.31	+1.80	+531.80
12	*inv*2L	$\mathrm{O}_{\mathrm{L1a}}$	+1.05	+1.53	+531.53
13	*inv*2L	$\mathrm{O}_{\mathrm{L1e2}}$	+0.04	+0.52	+530.52
13	*inv*2L	$\mathrm{O}_{\mathrm{L1e1}}$	+0.04	+0.52	+530.52

References

(1) Feller, D.; Peterson, K. A. Re-examination of Atomization Energies for the Gaussian-2 Set of Molecules. *J. Chem. Phys.* **1999**, *110*, 8384.

(2) Richter, N. A.; Kim, C.-E.; Stampfl, C.; Soon, A. Re-visiting the O/Cu(111) System-When Metastable Surface Oxides Could Become an Issue! *Phys. Chem. Chem. Phys.* **2014**, *16*, 26735.

(3) Soon, A.; Todorova, M.; Delley, B.; Stampfl, C. Oxygen Adsorption and Stability of Surface Oxides on Cu(111): A First-principles Investigation. *Phys. Rev. B* **2006**, *73*, 165424.

(4) Lee, T.; Lee, Y.; Piccinin, S.; Soon, A. Ab Initio Thermodynamics of Surface Oxide Structures under Controlled Growth Conditions. *J. Phys. Chem. C* **2017**, *121*, 2228–2233.

(5) Mándi, G.; Palotás, K. Chen's Derivative Rule Revisited: Role of Tip-Orbital Interference in STM. *Phys. Rev. B* **2015**, *91*, 165406.

(6) Biener, M. M.; Friend, C. M. Heteroepitaxial Growth of Novel MoO_3 Nanostructures on Au(111). *Surf. Sci.* **2004**, *559*, L173–L179.

(7) Biener, M. M.; Biener, J.; Schalek, R.; Friend, C. M. Growth of Nanocrystalline MoO_3 on Au(111) Studied by *In Situ* Scanning Tunneling Microscopy. *J. Chem. Phys.* **2004**, *121*, 12010–12016.

(8) Biener, M. M.; Biener, J.; Schalek, R.; Friend, C. M. Surface Alloying of Immiscible Metals: Mo on Au(111) Studied by STM. *Surf. Sci.* **2005**, *594*, 221–230.

(9) Guimond, S.; Göbke, D.; Sturm, J. M.; Romanyshyn, Y.; Kuhlenbeck, H.; Cavalleri, M.; Freund, H. J. Well-ordered Molybdenum Oxide Layers on Au(111): Preparation and Properties. *J. Phys. Chem. C* **2013**, *117*, 8746–8757.